Coexistence and interconvertibility of ferromagnetic and antiferromagnetic phases in the single crystal of Mn_3 single-molecule magnet

Yan Cui, Yan-Rong Li, Rui-Yuan Liu, Zhen-Yu Mi and Yun-Ping Wang
Beijing National Laboratory for Condensed Matter Physics, Institute of Physics, Chinese Academy of Sciences, Beijing 100190, People's Republic of China
(Dated: January 23, 2015)

We report the coexistence of ferromagnetic and antiferromagnetic phases in the single crystal of Mn_3 single-molecule magnet. The coexistent state appears within a certain period of time in the progress of either oxidation or reduction during a reversible oxidation-reduction process, when the sample is exposed in the air (oxygen) or the methyl vapor. We noticed an apparent change in the molecular structure, which is also reversible in terms of that the methyl group is dropped or added to the molecules during the oxidation or reduction. The absence or presence of the methyl group in the molecules exert an essential impact upon the intermolecular exchange interaction, and the ferromagnetic phase comes from the heterogenous intermolecular bonds between pairs of molecules of which one molecule has a methyl group whereas the other has lost the methyl group. The reversible change in molecular structure suggests the magnetic structure of Mn_3 might be designed and modulated at molecular scale, which implies Mn_3 has a great application potential.

PACS numbers: 75.50.Xx, 75.30.-m, 75.45.+j, 75.25.+z

The coexistence of multiple magnetic phases has attracted considerable interest in recent years, due to the potential for technological applications[1–3] and theoretical researches[4, 5]. In the reported researches, so far, the coexistent systems of multiple magnetic phases are polycrystals or crystals with apparent defects[1, 3, 6–8] in which the system structure as well as the mechanism of the formation of the coexistent state are complicated, making it difficult to anticipate feasible applications. In this paper, for the first time, we report the coexistence and interconvertibility of ferromagnetic (FM) and antiferromagnetic (AFM) phases in the single crystal of Mn_3 single-molecule magnet (SMM)[9–11] which is without apparent defect and displays quantum tunneling of magnetization (QTM) at low temperature[12, 13]. We have observed the coexistent state of FM and AFM phases during an oxidation process when the sample is preserved in the air or oxygen, as well as the reduction process when the oxidized sample is preserved in methanol gas. It is predicted that the oxidation-reduction process may be controlled by electrical stimuli[14] of scanning-tunneling-microscopy (STM) tip, which implies the magnetic structure may be designed at molecular scale, suggesting Mn_3 may have a great potential in extensive applications of nanodevices for magnetic storage and spintronics[15–19].

The single crystals of single-molecule magnet $Mn_3([Mn_3O(Et\text{-}sao)_3(ClO_4)(OH)_3])$ used in our experiment are synthesized according to the crystal growth procedures reported by Inglis et al[9]. Mn_3 is known to be a SMM with AFM intermolecular exchange interaction which only exists in ab plane with a honeycomb structure[11], and hence may be regarded as a two-dimensional magnetic system. The Hamiltonian of a Mn_3 molecule can be described as:

$$\hat{\mathscr{H}} = -D\hat{S}_z{}^2 + g\mu_0\mu_B\mathbf{H}\cdot\mathbf{S} - J\sum_{i=1}^{3}\hat{S}_{iz}\hat{S}_z, \qquad (1)$$

The first term represents the zero-field splitting energy, which produces a uniaxial anisotropy barrier separating degenerate opposite projections of the spin along the magnetic easy axis[12]. The second term is the Zeeman energy resulting from the interaction of the spin with an applied magnetic field. The third term is the intermolecular exchange interaction energy between one molecule and its three neighboring molecules.

The measurements are performed using 7T SQUID-VSM (Quantum Design), with three differently sized fresh samples preserved in the air or oxygen. The sizes of sample #1 to #3 are 2.0mm×2.0mm×0.8mm, 1.8mm×1.5mm×0.5mm, and 1.8mm×1.0mm×0.5mm, respectively. Each of the sample is well oriented and fixed on a home-made Teflon cubic, which is glued on the sample holder. The magnetic easy axis is ensured to be parallel to the applied field. Fig.1a presents the normalized magnetization vs temperature (M/M_s-T) curves of sample #1 preserved in the air on different days. It is seen that, FM phase starts appearing as time goes by, and becomes apparent on Day 10. In Fig.1b, the M/M_s-T curve at 1Oe indicates an apparent spontaneous magnetization at Tc=6.5K shown. The M/M_s-T curves of sample #1 on Day 10 shown in Fig.1b can be well fitted by $M(T,H) = k(T)H + C(T)$ at low magnetic fields, where the field-independent term $C(T)$ is from FM phase while the field-proportional term $k(T)H$ includes the contributions of AFM phase and a small amount of isolated FM occurrence. The fitting curves are indicated with the dash lines. It should be noted that, there is no field-independent term $C(T)$ when the field is applied perpendicular to the easy axis of the crystal while the magnetic moment of FM phase is parallel to the easy axis of the crystal. With the value of $C(T)$ at T=2K, the proportion of FM phase can be figured out. For all samples that we have measured, the proportion of FM phase is not more than 0.2%. Meanwhile, AFM phase is also observed by

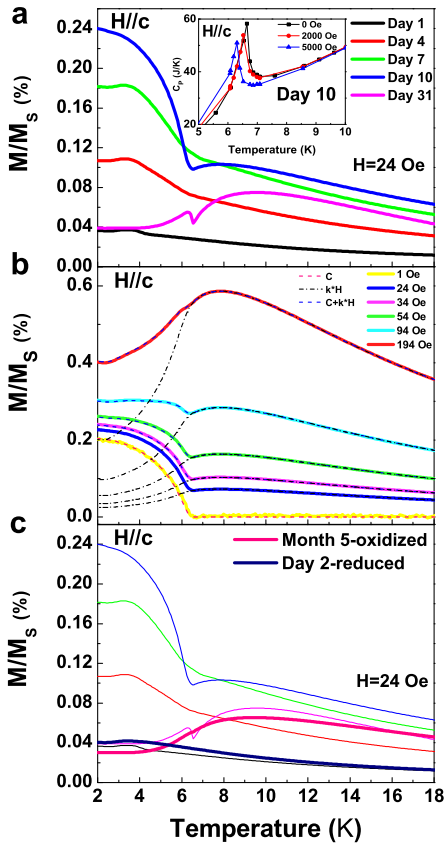

FIG. 1: (Color online) (a), The normalized magnetization vs temperature (M/M_s-T) curves of sample #1 preserved in the air on different days. The applied field is 24Oe. The inset shows the heat capacity (C_P) curves of sample #1 on the 10th day at different fields. (b), The M/M_s-T curves of sample #1 on the 10th day at different magnetic fields.They may be well fitted by $M(T,H) = k(T)H+C(T)$ marked by dash lines. (c), The M/M_s-T curves of the fully oxidized sample #3 before and after 24-hour reduction are presented in thick lines. The sample #3 is fully oxidized by being preserved in the air for 5 months. The applied field is 24Oe.

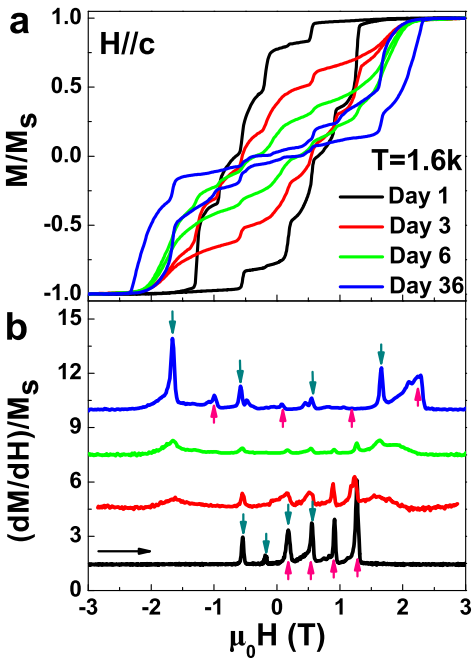

FIG. 2: (Color online) (a), Normalized magnetization hysteresis loops (M/M_s-H) of Mn_3 sample #2 preserved in the air on different days. The sweep rate is 50Oe/s. (b), Derivative curves from -3T to 3T which are shifted along y axis for clarity. The QTM peaks from |-6> to |6> and |-6> to |5> of Mn_3(I) (black line) and Mn_3(II) (blue line) are both indicated by dark cyan arrows and pink arrows, respectively.

heat capacity measurement which is performed on PPMS (Quantum Design). The inset in Fig.1a shows the heat capacity vs temperature curves of sample #1 at several given magnetic fields measured on Day 10. The peak moves to low temperature with increasing field, indicating the typical characteristic of AFM phase transition. Therefore, it is evident that FM and AFM phases coexist during the oxidation process.

The normalized magnetization hysteresis loops (M/M_s-H) on different days of sample #2 preserved in the air measured at T=1.6K and the derivatives of the M/M_s-H curves with increasing field in the loops are presented in Fig.2. Black loops/curves are of the fresh Mn_3 (hereafter Mn_3(I)), blue loops/curves are of the fully oxidized Mn_3 (hereafter Mn_3(II)), red and green loops/curves are of Mn_3 in the states between fresh and fully oxidized. In Fig.2a, the hysteresis loops become narrower as time goes by, indicating the anisotropy energy barrier is reducing. In Fig.2b, for the derivative curves, the magnetic moment is saturated at H_z=-3T, and the magnetic field is swept from -3T to 3T. It is seen that, the first QTM peak deviates from zero magnetic field, which is expected in the system with intermolecular-exchange-coupling [20]. The resonant field of the QTM from |-S> to |$S-l$> spin state in single-molecule magnets with identical exchange interaction can be described as[21]:

$$H_z = lD/g\mu_0\mu_B + (n_\downarrow - n_\uparrow)JS/g\mu_0\mu_B, \qquad (2)$$

where $n_\downarrow$ and $n_\uparrow$ represent the number of a tunneling molecule's neighboring molecules which occupy the |-6> and |6> state respectively.

Therefore, the series of QTM peaks of Mn_3(I) (black line) indicated by dark cyan arrows and pink arrows, originate from the QTM from |-6> to |6> and |-6> to |5> respectively. These peaks are succeeded by new series of QTM peaks (in the red, green and blue lines) as time goes by. The QTM from |-6> to |6> and |-6> to |5> of Mn_3(II) (blue line) are indicated by dark cyan arrows and pink arrows as well. Apparently, Mn_3(I) and Mn_3(II) molecules are coexistent during the oxidation process, as the QTM peaks of both Mn_3(I) and Mn_3(II) are observed in both red and green curves. On the other hand, the QTM peaks in all the curves are well defined, indicating that the easy magnetization axes of all the molecules are all parallel to the applied field, which means the sample

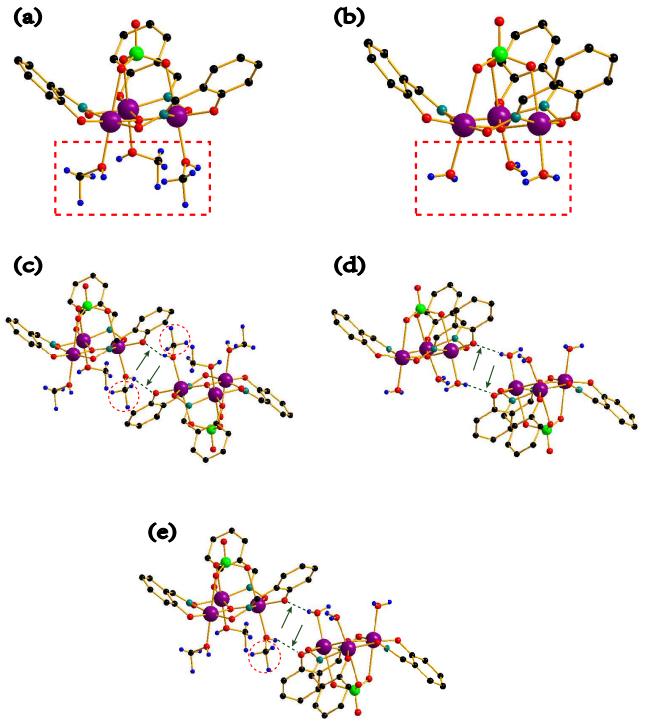

FIG. 3: (Color online) (a), molecule structure of Mn_3(I). (b), molecule structure of Mn_3(II). (c), hydrogen bonds between Mn_3(I) molecules. (d), hydrogen bonds between Mn_3(II) molecules. e, hydrogen bonds between Mn_3(I) molecule and Mn_3(II) molecule. Color code: Mn, purple; N, cyan; O, red; Cl, green; C, black; H, blue. The ethyl groups on Et-sao ligands are omitted for clarity. The hydrogen bonds are indicated by dark green arrows. The methyl groups near the hydrogen bonds are circled by red dashes.

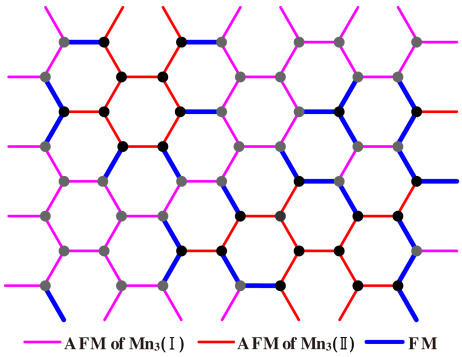

FIG. 4: (Color online) Sketch map of magnetic structure in ab plane of Mn_3 during the oxidation process. Gray dots represent Mn_3(I) molecules. Black dots represent Mn_3(II) molecules. The intermolecular exchange interaction only exists in ab planes. Magenta lines represent the intermolecular bonds with AFM exchange interaction between Mn_3(I) molecules. Red lines represent the intermolecular bonds with AFM exchange interaction between Mn_3(II) molecules. Blue lines represent the intermolecular bonds with FM exchange interaction between Mn_3(I) molecules and Mn_3(II) molecules.

is still a single crystal as the orientation remains the same during the oxidation process. According to equation (2), the value of anisotropy parameter D and intermolecular interaction J for Mn_3(I) and Mn_3(II) may be calculated out respectively. For Mn_3(I), D=0.98K, J=-0.041K; and for Mn_3(II), D=0.925K, J=-0.132K. The negative value of J indicates the AFM exchange interaction in both Mn_3(I) and Mn_3(II). The AFM coupling parameter J of Mn_3(II) is over three times of Mn_3(I), and the coupling has contributed to the AFM phase transition observed in the inset of Fig.1a. It should be noted that, FM phase also appears in the same period of time during the process, but since it has a low concentration in the sample, the QTM peaks of FM phase are not observed.

We've also observed that, another fresh sample (sample #3) becomes fully oxidized after it is preserved in the air for 5 months, with the proportion of FM phase not more than 0.001%. Remarkably, this oxidized sample turns back to the fresh sample when it is preserved in methanol gas (0.10bar) for more than 24 hours, which indicates the oxidation process can be reversed. M/M_s-T curves of sample #3 before and after the reduction process are shown in Fig.1c. The M/M_s-T curves of sample #3 right after the 24-hour reduction is close to that of sample #1 on Day 1. Since oxygen seems to play a key role in the process, a new fresh sample is preserved in oxygen for further test, and it is seen that, the M/M_s-T curve on Day 6 is similar to that of sample #1 on Day 31 in Fig.1a which is preserved in the air. The result indicates that the oxidation process is accelerated by oxygen. Additional experiments with the fresh samples preserved in argon or nitrogen for two weeks and covered by AB glue for one year indicate that, the M/M_s-T curves of these samples remains unchanged when the samples are isolated from oxygen and methanol gas. Therefore, it is safe to conclude that, the oxidation-reduction process may be manually controlled by favorably applying either oxygen or methanol gas to the sample to obtain the desired magnetic state of the sample.

In order to understand the nature of the magnetic characteristics during this process, we have monitored the crystal structure[9] of the sample before and after the oxidation. The crystal structures of fresh and fully oxidized samples are characterized by four-circle X-ray diffractometer (Bruker SMART APEX-CCD) and the molecule structures are figured out by SHELXTL. The lattice structure and space group of the sample before and after the oxidation remain the same. The only apparent change seen in Fig.3a and Fig.3b is that, each Mn_3(II) molecule has lost three methyl groups. The lattice constant only differs slightly with this change. For both Mn_3(I) and Mn_3(II), two intermolecular hydrogen bonds[9] are formed between the oxygen and hydrogen atoms as shown in Fig.3c and Fig.3d, and these intermolecular hydrogen bonds determines the intermolecular exchange interaction. The presence or absence of methyl

groups results in obvious changes of the distance and the angle of these hydrogen bonds, and hence significantly affects the magnitude and even the sign of the intermolecular exchange interaction parameter J[10, 20, 22].

With regard to FM phase observed in the process, it may be well understood as the following. As shown in Fig.4, the fresh sample is soaked in the oxygen, and hence, the Mn_3(I) molecules have the probability to be oxidized which results in the random distribution of Mn_3(II) molecules. Black dots connected by red lines represent Mn_3(II) molecules with strong AFM exchange interaction (J=-0.132K) which is the origin of the AFM phase, whereas the grey dots connected by magenta lines represent Mn_3(I) molecules which are not oxidized and hence with weak AFM interaction (J=-0.041K). The blue lines indicate the heterogenous intermolecular bonds (HIBs) between Mn_3(I) and Mn_3(II) molecules (each HIB between the two different molecules consists of two hydrogen bonds connecting the two molecules as shown in Fig.3e). As mentioned above, the sample always maintains the monocrystalline structure. Therefore, it may be convinced that the FM phase observed during the process should come from the HIBs between Mn_3(I) and Mn_3(II). The presence of FM phase indicates that the exchange interaction[10, 20, 22] between Mn_3(I) and Mn_3(II) (shown in Fig.3e) is FM interaction (J>0). In actual scenario, there are relatively fewer HIBs with FM interaction at the beginning of the process, these HIBs appear in small proportion, isolated and noncoherent. With the oxidation process developing, there are more and more HIBs appearing, and some of them will correlate with each other by dipolar interaction to form "pieces" of FM phase which will gradually accumulate and then the FM phase will become manifested. Meanwhile, there are some area that most Mn_3(I) molecules in it are oxidized, hence the AFM phase is formed in these area. After that, the FM phase will gradually diminish and disappear when more and all molecules become oxidized eventually, and the sample will exhibit only antiferromagnetism in the end. On the other hand, when the oxidized sample is preserved in methanol gas, the methyl groups of methanol will graft on Mn_3(II) molecules, then a reduction process will take place, the oxidized sample will change back to the fresh sample.

It is very clear, the oxidation-reduction process is essentially of that, the Mn_3 molecule loses or gains methyl groups. We have demonstrated that the process is reversible, and may be controlled by chemical stimuli of applying favorably oxygen or methanol gas to the sample so that the methyl groups may be added to or dropped from the Mn_3 molecule. It might be also possible that, the process could be controlled by photo-irradiation[23] or even electrical stimuli [14]. We are especially attracted to the thought of electrical stimuli, with the idea of grafting the monomolecular layer or thin film of Mn_3 on conducting substrate (the method which has been tried for Mn_3[24]), placing the device in a mixture of oxygen and methanol gas with proper dosage, and setting a local voltage between a STM tip and the conducting substrate to determine oxidation or reduction process so that the intermolecular exchange interaction may be switched between FM and AFM by tuning the voltage, which implies the magnetic structure of Mn_3 may be designed or modified at molecular scale. This also suggests a possibility of extending single-molecule spintronics device[15, 19] to two-dimensional spintronics device as the magnetic coupling network may be modulated as desired.

This work was supported by the National Key Basic Research Program of China (grant 2011CB921702).

[1] Y. Murakami, J. H. Yoo, D. Shindo, T. Atou and M. Kikuchi, Nature **423**, 965 (2003).
[2] A. Moreo, M. Mayr, A. Feiguin, S. Yunoki, and E. Dagotto, Phys. Rev. Lett. **84**, 5568 (2000).
[3] B. Barbara and M. F. Rossignol, Phys. Rev. Lett. **45**, 938 (1980).
[4] M. A. Santos, M. C. Marques, and J. M. B. Oliveira, J. Phys. C: Solid State Phys. **21**, 747 (1988).
[5] O. V. Yazyev and L. Helm, Phys. Rev. B **75**, 125408 (2007).
[6] A. Moreo, S. Yunoki and E. Dagotto, Science **283**, 2034 (1999).
[7] L. Chen, et al. Sci. Rep. **3**, 2599; DOI:10.1038/srep02599 (2013).
[8] Z. R.Wang, X. L. Wang, J. A. Fernandezbaca, D. C. Johnston and D. Vaknin, Science **264**, 402 (1994).
[9] R. Inglis, G. S. Papaefstathiou, W. Wernsdorfere and E. K. Brechin, Aust. J. Chem. **62**, 1108 (2009).
[10] R. Inglis,et al. Dalton Trans., 9157 (2009).
[11] R. Inglis, et al. Chem. Commun., 5924 (2008).
[12] J. R. Friedman, M. P. Sarachik, J. Tejada, and R. Ziolo, Phys. Rev. Lett. **76**, 3830 (1996).
[13] L. Thomas, et al. Nature **383**, 145 (1996).
[14] L. W. Liu, et al. Sci. Rep. **3**, 1210; DOI: 10.1038/srep01210 (2013).
[15] W. J. Liang, M. P. Shores, M. Bockrath, J. R. Long and H. Park, Nature **417**, 725 (2002).
[16] L. Bogani and W. Wernsdorfer, Nat. Mater. **7**, 179 (2008).
[17] S. D. Jiang, G. Karin, C. Christian, and B. Lapo, Sci. China-Chem. **55**, 867 (2012).
[18] M. Lee, T. Jonckheere, and T. Martin, Phys. Rev. Lett. **101**, 146804 (2008).
[19] M. H. Jo, et al. Nano Lett. **6**, 2014 (2006).
[20] C. Boskovic, et al. J. Am. Chem. Soc. **125**, 14046 (2003).
[21] Y. R. Li, R. Y. Liu, H. Q. Liu and Y. P. Wang, Phys. Rev. B **89**, 184401 (2014).
[22] R. K. Nesbet, Phys. Rev. **122**, 1497 (1961).
[23] H. Miyasaka and M. Yamashita, Dalton Trans., 399 (2007).
[24] A. Naitabdi, J. P. Bucher, P. Gerbier, P. Rabu and M. Drillon, Adv. Mater. **17**, 1612 (2005).